Robust delayed resonator with acceleration feedback – design by double root assignment and experimental validation

Matěj Kuře, Jaroslav Bušek, Islam Boussaada, Wim Michiels, Silviu-Iulian Niculescu, Tomáš Vyhlídal

HAL Id: hal-04409473
https://hal.science/hal-04409473

Submitted on 22 Jan 2024

Robust delayed resonator with acceleration feedback – design by double root assignment and experimental validation

Matěj Kuře[a], Jaroslav Bušek[a], Islam Boussaada[b], Wim Michiels[c], Silviu-Iulian Niculescu[b], Tomáš Vyhlídal[a]

[a]*Faculty of Mechanical Engineering, and Czech Institute of Informatics, Robotics and Cybernetics, Czech Technical University in Prague, Jugoslávských partyzánů 1580/3, 160 00 Praha 6, Czech Republic,* `Tomas.Vyhlidal@cvut.cz`
[b]*Université Paris-Saclay, CNRS, CentraleSupélec, Laboratoire des signaux et systèmes, Inria, Inria Saclay-Île-de-France, 91190, Gif-sur-Yvette, France, France,* `{Islam.Boussaada, Silviu.Niculescu}@l2s.centralesupelec.fr`
[c]*Department of Computer Science, KU Leuven, Celestijnenlaan 200A, B-3001 Heverlee, Belgium,* `Wim.Michiels@cs.kuleuven.be`

Abstract

A combination of analytical and numerical time-delay-system spectrum-shaping tools are applied to the design of the robust delayed resonator with an acceleration feedback. First, the delayed resonator model is turned into a dimension-less form with the objective to generalize the derived results. The main theoretical result is then provided as a complete parameterization of the proposed resonator feedback with two delay terms to assign a pair of roots with multiplicity two on the imaginary axis. In the frequency-domain, the double roots are projected to widening the stop-band in the active absorber frequency response, which increases its robustness in vibration suppression. On the other hand, they have a destabilizing effect on the overall system dynamics. The stabilization is subsequently performed by an additional controller via spectral optimization. The design is thoroughly validated by both simulations and experiments where the results are compared with the classical delayed resonator with lumped delay acceleration feedback.

Keywords: Double root assignment, active vibration control, robust control, acceleration feedback, spectral method, delayed resonator

1. Introduction

Passive as well as actively tuned vibration absorbers have become established tools in the vibration suppression task. The passive absorbers are easy to apply, but their applicability is limited to a narrow range close to the absorber natural frequency [1]. Besides, due to inherent damping and friction forces in their flexible links, the vibration suppression cannot be ideal. The applicable frequency range can be extended and vibration absorption quality can be enhanced by active tuning of the absorber properties. It can be done mechanically by adjusting the absorber mass, stiffness or damping, see e.g. [2, 3, 4]. However, considerably better performance can be achieved if the absorber is actively actuated [1]. The *delayed resonator* (DR) concept proposed in 1990s by N. Olgac and his co-workers is a typical example of actively tuned vibration absorber. Next to becoming an established tool for vibration suppression, it has become one of the typical examples of benefits of time delays in vibration suppression applications. The time-delay feedback

is applied to modify the active absorber properties resulting in the entire suppression of undesirable oscillations. The absorber is tuned to an ideal resonator, marginally stable, where the DR acts as a perfect resonator and absorbs the vibrations entirely.

The first concepts of DR used delayed feedback from absolute position of the absorber [5], [6]. Consequently a relative position of the absorber with respect to the primary structure was applied [7]. A damped centrifugal DR with angular position feedback with variable gain and time delay was considered in [8]. After these first results, including also extension to delayed velocity feedback [9], [10], the research mainstream of the DR analysis and design switched to delayed feedback from acceleration sensor mounted on the absorber. This had a practical motivation as the accelerometers are easy to apply and of relatively low cost. To the best of the authors' knowledge, the DR with acceleration feedback was first introduced in [11], where the DR based absorption methods were implemented on a distributed parameter structure under high frequency excitation. Research in DR with acceleration feedback then followed in many directions. An algorithm for multi-degree of freedom (MDOF) mechanical structures with multiple DRs is described in [12]. In [13], an automatic tuning method of the DR was proposed to handle parametric uncertainties. An auto-tuning algorithm to enhance the robustness against uncertainties was proposed in [14], see also [15] for parameter identification and re-tuning the delayed feedback, and [16] for sensitivity analysis and parameter optimization.

In the past decade, delayed resonator feedback was studied by a broader authors' team of this paper. A complete dynamics analysis of a DR with acceleration feedback was performed in [17] revealing an unfavorable neutral[1] character of spectral properties of the DR. In order to mitigate this undesirable effect, an alternative distributed delay resonator was proposed and analyzed in [20], resulting in retarded spectral properties. By applying the method of *Cluster Treatment of Characteristic Roots* [21], it was also shown in [17] and [20] that the operable frequency range is limited regardless the DR feedback type. From below, it is limited by the stability boundary, while the delay implementation aspects limit the range from the above - due to the exponential decay of the delay length with respect to growing frequency. A methodology for further extension of the operable frequency range of the DR with acceleration feedback was proposed in [22], see also recent work [23]. It is based on extending the feedback by a delay free factor virtually modifying the mass of the absorber and thus its natural frequency. Besides, implementation aspects of the resulting, so-called *extended delay resonators* have been discussed.

The analysis performed in [17] and [20] for DR with the acceleration feedback was extended to DR with position or velocity feedback in [24]. As pointed out, if not tuned properly, the DR can considerably lower the stability margin or even destabilize the system. Besides, the needed force and power of the DR for entire vibration of the primary were derived, which are independent of the DR type. As one of the main results, it was also demonstrated that the existing DR solutions suffer from extreme fragility in vibration suppression taking into account mismatch between the design and true excitation frequencies. Following from the frequency domain analysis, the entire vibration suppression only takes place if the resonant frequency adjusted by the resonator feedback is equal to the true excitation frequency. The performance of the resonator decays considerably

---

[1] For an appropriate definition of the neutral functional differential equations and their properties, we refer to [18, 19] and the references therein.

even for very small differences in these frequencies.

Recent works of DR with acceleration feedback include also the work reported in [25], where the mechanical absorber structure is replaced by an electrical circuit that resonates. In [26], [27], a challenging problem of non-collocated vibration absorption by DR was opened and analysed. The work [28] supplements the DR with an amplifying mechanism. An interesting study on generalizing the DR towards fractional derivative feedback was recently presented in [29]. Let us also mention the approach of [30] combining position and velocity feedback, the work reported in [31] targeting multiple-frequencies by multi-parameter delayed position feedback and [32], [33] extending the DR concept to two-dimensional vibration absorption using delayed position feedback at the three actuators of the 2D absorber. Motivated by DR applications, in [34], stability analysis of systems with delayed position and velocity was performed. Regions in the feedback gain parameters were determined to assure delay-dependent exponential stability.

In [35] a delay-free PI acceleration feedback of the absorber was proposed. However, due to risky noise integration phenomenon, the feedback needs to be supplemented with high-pass filters, which makes the overall feedback more complex compared to time delay feedback. The stability of the vibration absorber using acceleration and displacement feedback was analyzed in [36] utilizing the Nyquist criterion. The work [37] provides analysis of a primary structure and piezoelectric based dynamic vibration absorber. The active feedback is taken from the acceleration of the primary mass.

As mentioned above, and addressed thoroughly in [24], the main drawbacks of the classical DR applications are: i) extreme fragility in vibration suppression with respect to mismatch between the design and true excitation frequency, and ii) destabilizing effect of the DR deployment to the primary structure. Thus, the main objective of this paper is to propose a method for a straightforward design of a robust DR with acceleration feedback. The first work in this direction is [38], where the DR feedback design is formulated as an optimization problem over the parameter set formed by the polynomial coefficients. The objective was to minimize the sensitivity of the resonator performance with respect to variations of the excitation frequency considering a system stability constraint. The arising non-convex and non-smooth optimization problem is widely discussed and a penalty method is developed, where the unconstrained problem is solved using available software tools for optimization and spectral design of time delay systems. In this paper, we utilize recent results on admissible multiplicity of fixed structure delay systems as in [39, 40, 41], which leads to much simpler design rules and feedback structure of the DR compared to [38]. Analogously to [38], the stabilization of the overall system is addressed, here by a supplementary finite order controller stabilizing the platform with a robust feedback through an additional actuator. For the controller tuning, the procedure synthesized in [42] and implemented in the software package `TDS-CONTROL` [43] is applied. As a preliminary step, the stability posture of the robust DR is analysed. To demonstrate the practical applicability of the method, an experimental validation of the overall control scheme is performed on a mechatronic system actuated by linear voicecoils and governed by an industrial controller.

The paper extends preliminary results presented in a conference publication [44]. Compared to a single parameter set leading to a double root derived in [44], an infinite number of parameter sets leading to a double root is presented. Additionally, an enhanced attention is paid to the stability aspects and experimental validation. The paper is organized as follows. In Section 2, the concept of vibration absorber and functioning of the overall
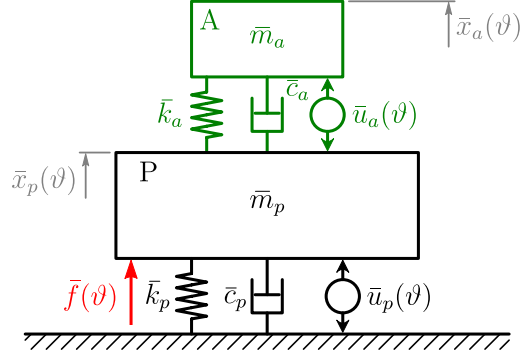
3

Figure 1: Primary Structure (P) with an active vibration absorber (A) to suppress displacement $\bar{x}_p$ induced by harmonic disturbance force $\bar{f}(t)$.

set-up including a stabilizing controller is outlined. Section 3 then provides the main result with introducing the robust delayed resonator concept and providing analytic rules for double root assignment. Next, the design of the additional finite order controller is addressed together with its parametrization by minimizing the spectral abscissa. Both simulation and experimental validation of the proposed concept are done in Section 4, where the robust DR performance is compared with the performance of classical delayed resonator concept. In Section 5, the conclusions are given.

2. Problem statement and preliminaries

Consider the mechanical configuration of the platform P and active absorber A as shown in Fig. 1. The position of the primary structure and the position of the absorber are denoted by $\bar{x}_p$ and $\bar{x}_a$, respectively. The physical parameters of the setup are the masses of the platform and absorber bodies $\bar{m}_p, \bar{m}_a$, the damping $\bar{c}_p, \bar{c}_a$, and the stiffness $\bar{k}_p, \bar{k}_a$ of the links. The platform is excited by a harmonic force

$$\bar{f}(\vartheta) = \bar{f}_a \cos(\bar{\omega}_f (1 + \delta)\vartheta), \tag{1}$$

where ϑ is time, $\bar{f}_a$ is the amplitude, $\bar{\omega}_f$ is the nominal excitation frequency and δ denotes its deviation in relative sense (satisfying $|\delta| < 1$). Thus, the perturbed excitation frequency is given as $\bar{\omega} = \bar{\omega}_f(1 + \delta)$. The control objective is to introduce an active actuation force $\bar{u}_a$ in order to fully suppress the vibration of the primary structure ($\bar{x}_p$) in a robust way, i.e. with low sensitivity to the frequency deviation δ. In order to stabilize and enhance the robustness of the overall system, additional control force $\bar{u}_p$ is available.

2.1. Dimensionless model

For the generalization purposes, the model of the setup is derived in the dimensionless form. Considering $\bar{x}_p = 0$, the isolated absorber can be described by

$$\ddot{\bar{x}}_a(\vartheta) + 2\zeta\Omega\dot{\bar{x}}_a(\vartheta) + \Omega^2\bar{x}_a(\vartheta) = \frac{1}{\bar{m}_a}\bar{u}_a(\vartheta), \tag{2}$$

where $\Omega = \sqrt{\frac{\bar{k}_a}{\bar{m}_a}}$ is the natural frequency and $\zeta = \frac{\bar{c}_a}{2\sqrt{\bar{m}_a\bar{k}_a}}$ is the damping of the passive absorber. Scaling the time ϑ with respect to the frequency Ω, i.e., by introducing

4

dimensionless time $t = \Omega\vartheta$, and setting

$$x_a(t) = \bar{x}_a(\vartheta), \ u_a(t) = \frac{1}{\bar{m}_a\Omega^2}\bar{u}_a(\vartheta), \ \text{with } \vartheta = \frac{t}{\Omega},$$

we obtain an isolated active absorber form

$$\ddot{x}_a(t) + 2\zeta\dot{x}_a(t) + x_a(t) = u_a(t), \tag{3}$$

with the only parameter ζ.

Applying the same scaling of variables and time to the overall set-up according to Fig. 1 and setting $x_p(t) = \bar{x}_p(\vartheta)$, we obtain

$$\begin{cases} \ddot{x}_a(t) + 2\zeta\dot{x}_a(t) + x_a(t) - 2\zeta\dot{x}_p(t) - x_p(t) = u_a(t), \\ m_p\ddot{x}_p(t) + (2\zeta + c_p)\dot{x}_p(t) + (1 + k_p)x_p(t) - 2\zeta\dot{x}_a(t) - x_a(t) = -u_a(t) + u_p(t) + f(t), \end{cases} \tag{4}$$

where $m_p = \frac{\bar{m}_p}{\bar{m}_a}, c_p = \frac{\bar{c}_p}{\bar{m}_a\Omega}, k_p = \frac{\bar{k}_p}{\bar{m}_a\Omega^2}$ are the scaled mass, the damping and the stiffness parameters of the primary structure, u_p is defined as $u_p(t) = \frac{1}{\bar{m}_a\Omega^2}\bar{u}_p(\vartheta)$, with $\vartheta = t\Omega$, while the scaled excitation force is given by

$$f(t) = \frac{1}{\bar{m}_a\Omega^2}\bar{f}(\vartheta). \tag{5}$$

2.2. Unifying excitation frequency with absorber natural frequency

Without loss of generality, we assume that the excitation frequency $\bar{\omega}_f$ in (1) is unified with the natural frequency of the absorber Ω, i.e. $\bar{\omega}_f = \Omega$. In this way, the force term in (4) becomes $f(t) = \frac{\bar{f}_a}{\bar{m}_a\Omega^2}\cos((1+\delta)t)$. The unification of these frequencies can be achieved by modifying the physical parameters of the absorber. In particular, a modification of the mass is an easy task to do leading to

$$\bar{m}_a(\bar{\omega}_f) = \frac{\bar{k}_a}{\bar{\omega}_f^2}. \tag{6}$$

Alternatively, as shown in [22], extending the resonator feedback by a delay-free acceleration term

$$\bar{u}_a(\vartheta) = -h\ddot{\bar{x}}_a(\vartheta) + \bar{v}_a(\vartheta), \tag{7}$$

with a parameter h and a new input $\bar{v}_a$, allows virtual modification of the absorber mass from $\bar{m}_a$ to $\bar{m}_a + h$. The unification of the excitation and natural frequencies implies

$$h(\bar{\omega}_f) = \frac{\bar{k}_a}{\bar{\omega}_f^2} - \bar{m}_a. \tag{8}$$

For practical aspects and limitations of this approach we refer the reader to [22].

2.3. Active feedback to achieve ideal uni-frequency absorber

The structural analysis with the aim to achieve complete vibration suppression and stability posture is performed in the Laplace transform forms of the model and the controllers. A generalized absorber active feedback assumed in the form

$$U_a(s) = P(s)X_a(s), \tag{9}$$

with transfer function $P(s)$ is applied to turn the physical absorber to an ideal absorber which entirely absorbs the vibration at excitation frequency $\omega_f = 1$. For stabilizing purposes, the primary structure is equipped with an active feedback

$$U_p(s) = K(s) X_p(s),\tag{10}$$

with controller $K(s)$, which can be used for platform positioning or just for improving the overall dynamical properties in vibration suppression. The model (4) is transformed into

$$\begin{cases} R(s)X_a(s) - H(s)X_p(s) = U_a(s), \\ Z(s)X_p(s) - H(s)X_a(s) = -U_a(s) + U_p(s) + F(s), \end{cases}\tag{11}$$

with $R(s) = s^2 + 2\zeta s + 1$, $Z(s) = m_p s^2 + (2\zeta + c_p)s + (1 + k_p)$, and $H(s) = 2\zeta s + 1$. Substituting (9) and (10) into (11), the transfer function between the excitation force f and the position of the primary structure x_p is then given by

$$G_{f,x_p}(s) = \frac{X_p(s)}{F(s)} = \frac{R(s) - P(s)}{(R(s) - P(s))(Z(s) - K(s)) + (P(s) - H(s))H(s)}.\tag{12}$$

If the transfer function $P(s)$ is parameterized so that the characteristic equation of the resonator composed of the absorber (3) and the feedback (9), given by

$$M(s) = R(s) - P(s) = 0,\tag{13}$$

has a root couple $s_{1,2} = \pm j\omega_f$, composing a pole couple of the resonator, then

$$G_{f,x_p}(j\omega_f) = 0,\tag{14}$$

indicating that no vibration at the given frequency $\omega = \omega_f$ is transferred in this f to x_p channel and the vibration is ideally suppressed. Note however that including the resonator feedback affects the dynamical properties of the entire system, which are determined by the roots of the characteristic equation

$$(R(s) - P(s))(Z(s) - K(s)) + (P(s) - H(s))H(s) = 0.\tag{15}$$

Assuming the presence of the delay terms in $P(s)$, equation (15) has in general infinitely many roots. For the stability implications, all of them need to be located safely in the left half of the complex plane.

3. Main result - Robust resonator feedback design

The resonator feedback is considered in the form

$$u_a(t) = \int_0^t \alpha_0 \ddot{x}_a(\theta) + \alpha_1 \ddot{x}_a(\theta - \tau_1) + \alpha_2 \ddot{x}_a(\theta - \tau_2)\, d\theta,\tag{16}$$

with delays $\tau_2 > \tau_1 > 0$ and parameters $\alpha_0, \alpha_1, \alpha_2$ satisfying

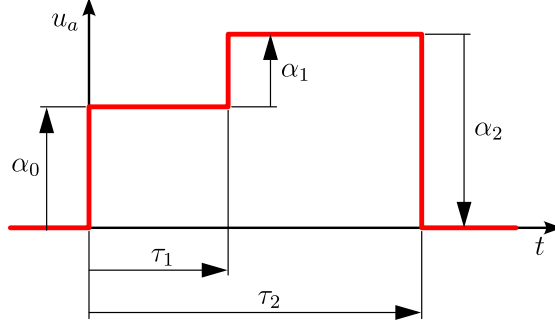$$\sum_{i=0}^{2} \alpha_i = 0,\tag{17}$$

6

Figure 2: Impulse response of the distributed delay used in the resonator feedback (16), considering the measured acceleration $\ddot{x}_a$ as the input while satisfying (17).

which imposes a finite length of the impulse response from $\ddot{x}_a$ to u_a. The role of the gains and delays in (16) is shown in Fig. 2, where an impulse response of the distributed delay is shown, taking $\ddot{x}_a$ as the input. As can be seen, τ_1 determines the length of the first pulse, while the overall length is determined by τ_2. The gains α_i, $i = 0..2$ then determine the magnitude distribution of the pulses. Taking into consideration the feedback transfer function form

$$P(s) = \frac{\alpha_0 + \alpha_1 \mathrm{e}^{-s\tau_1} + \alpha_2 \mathrm{e}^{-s\tau_2}}{s} s^2, \tag{18}$$

the characteristic equation (13) of the delayed resonator composed of the absorber (3) and active feedback (16) is then given

$$M(s) = s^2 + \left(2\zeta - \alpha_0 - \alpha_1 \mathrm{e}^{-s\tau_1} - \alpha_2 \mathrm{e}^{-s\tau_2}\right) s + 1. \tag{19}$$

Notice that despite the involved acceleration feedback, due to the distributed delay nature, the characteristic equation structure indicates the presence of a point spectrum (*retarded* case), [20].

3.1. DR parameterization by assigning a double root

   The objective in the design of the robust resonator is to widen the frequency stopband of $|G_{f,x_p}(j\omega)|$ in the vicinity of $\omega = 1$. This can be done by assigning a double root $s_{1,2} = j$ to the characteristic equation of the delayed resonator (19), which appears in the numerator of (12).

Theorem 1. *For a given damping factor $\zeta \in [0,1]$, under the design condition (17), the multiplicity of $s_{1,2} = j$ as a root of (19) cannot exceed 2. The required multiplicity 2 is reached if and only if, for arbitrary positive integers k_1 and k_2 satisfying $k_1 \neq k_2$ and at least one of them being odd, the parameters of the resonator's feedback are given by*

$$\begin{cases} \tau_1 = k_1 \pi, \\ \tau_2 = k_2 \pi, \\ \alpha_0 = -\dfrac{2}{\pi} \dfrac{(1 + \pi k_2 \zeta)(-1)^{k_1+k_2} - \pi k_1 \zeta - 1}{k_1 + (k_2 - k_1 - k_2(-1)^{k_1})(-1)^{k_2}}, \\ \alpha_1 = \dfrac{2}{\pi} \dfrac{(-1)^{k_1}((-1)^{k_2} + \pi(-1)^{k_2} k_2 \zeta - 1)}{k_1 + (k_2 - k_1 - k_2(-1)^{k_1})(-1)^{k_2}}, \\ \alpha_2 = -\dfrac{2}{\pi} \dfrac{\pi k_1 \zeta - (-1)^{k_1} + 1}{k_1 + (k_2 - k_1 - k_2(-1)^{k_1})(-1)^{k_2}}. \end{cases} \tag{20}$$

7

Proof. Substituting $s = j$ in the quasipolynomial function (19) as well as its first derivative and separating the real and imaginary part, we get the following system of four trigonometric polynomials

$$\begin{cases} -\alpha_1 \sin(\tau_1) - \alpha_2 \sin(\tau_2) = 0, \\ (2\zeta - \alpha_0) - \alpha_1 \cos(\tau_1) - \alpha_2 \cos(\tau_2) = 0, \\ \alpha_1 \tau_1 \sin(\tau_1) + \alpha_2 \tau_2 \sin(\tau_2) + (2\zeta - \alpha_0) - \alpha_1 \cos(\tau_1) - \alpha_2 \cos(\tau_2) = 0, \\ 2 + \alpha_1 \tau_1 \cos(\tau_1) + \alpha_2 \tau_2 \cos(\tau_2) + \alpha_1 \sin(\tau_1) + \alpha_2 \sin(\tau_2) = 0. \end{cases} \quad (21)$$

From the first two equations we eliminate the trigonometric functions in τ_1

$$\begin{cases} \sin(\tau_1) = -\dfrac{\alpha_2 \sin(\tau_2)}{\alpha_1}, \\ \cos(\tau_1) = -\dfrac{-2\zeta + \alpha_0 + \alpha_2 \cos(\tau_2)}{\alpha_1}, \end{cases} \quad (22)$$

which after being substituted in the remaining two equations of (21) gives

$$\begin{cases} \sin(\tau_2) = 0, \\ \cos(\tau_2) = \dfrac{\tau_1 (2\zeta - \alpha_0) + 2}{\alpha_2 (\tau_1 - \tau_2)}. \end{cases} \quad (23)$$

Substituting again (23) in (22) allows us to prove that

$$\tau_1 = k_1 \pi \quad \text{and} \quad \tau_2 = k_2 \pi, \quad (24)$$

where k_1 and k_2 are positive integers.

Substituting the obtained values of τ_1 and τ_2 and $s = j$ in the expression of $M(s)$ as well as in the expression of $M'(s)$ one obtains:

$$\begin{cases} -j \left(-2\zeta + \alpha_0 + \alpha_1 (-1)^{-k_1} + (-1)^{k_2} \alpha_2 \right) = 0, \\ 2\zeta - \alpha_0 - \alpha_1 (-1)^{-k_1} - (-1)^{k_2} \alpha_2 + j \left(2 + \alpha_1 k_1 \pi (-1)^{-k_1} + (-1)^{k_2} \alpha_2 k_2 \pi \right) = 0, \end{cases} \quad (25)$$

which gives

$$\alpha_1 = -\frac{2 + (2\zeta - \alpha_0) k_2 \pi}{(-1)^{-k_1} \pi (k_1 - k_2)}, \quad \alpha_2 = \frac{2 + (2\zeta - \alpha_0) k_1 \pi}{(-1)^{k_2} \pi (k_1 - k_2)}. \quad (26)$$

Solving the set of equations (17) and (26) gives (20). To prove that the maximal multiplicity of $s = j$ as a root of (19) is two, one can substitute the obtained parameter values in equation $M''(j) = 0$, leading to an inconsistency. $\qquad \square$

Remark 2. *As stated in the theorem, the only possible control laws of the form (16) feature delays $\tau_1 = k_1 \pi$ and $\tau_2 = k_2 \pi$ with either (k_1, k_2) both odd, or one of them even and the other one odd. One may wonder about a physical interpretation for the exclusion of possibilities with k_1 and k_2 both even. If both were even, the controller's transfer function would satisfy*

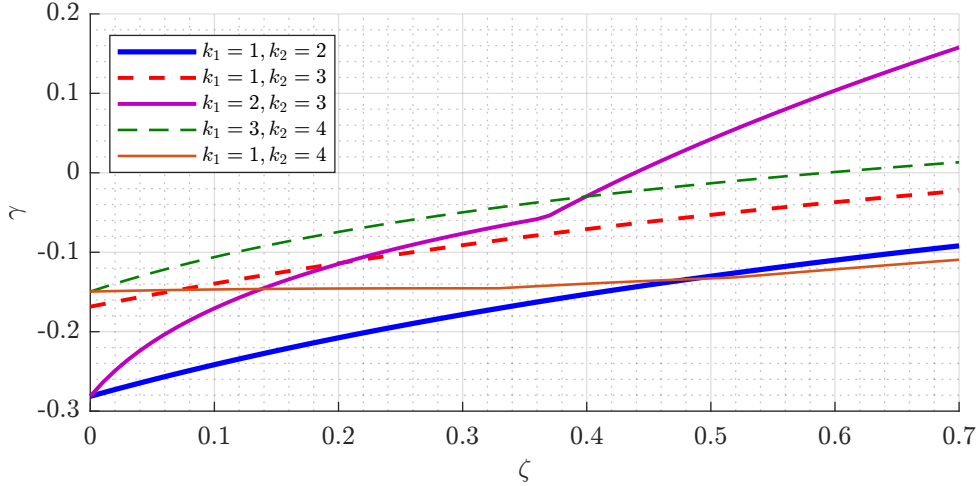$$P(j) = j (\alpha_0 + \alpha_1 + \alpha_2) = 0$$

Figure 3: Real part of the drDR non-assigned rightmost root with respect ζ and k_1, k_2.

in view of (17), *i.e., a harmonic function of frequency equal to one would be filtered out by the control. Hence, the damping of the absorber, having (modified) natural frequency one, cannot be compensated. Note that control law (16) can be interpreted as a generalization of Pyragas type feedback (also called time-delayed feedback). This type of feedback has originally been developed for nonlinear systems, where the filtering property induced by time-shifted differences is employed to preserve the shape of a periodic orbit with given period or an equilibrium's position to be stabilized [45]. In [46, Figure 2.3] the impact of the filtering property on the stabilizabilty of linear second-order systems is highlighted.* □

Remark 3. *Notice that the multiplicity of a given root of a quasipolynomial is bounded by the generic Polya and Szegö bound denoted PS_B, see for instance [47, 39]. Such a bound is defined in [39] as the degree of the quasipolynomial and corresponds to the sum of the involved polynomials' degrees plus the number of delays. In [41], it is shown that the multiplicity of purely imaginary roots (with a non-vanishing frequency) of a generic quasipolynomials never reaches PS_B and a sharper bound for its admissible multiplicities is established. Accordingly, the degree of the quasipolynomial $M(s)$ defined by (19) is 6. In particular, a characteristic root located on the real (or imaginary) axis may have the maximal multiplicity equal to 6 (or 3). However, in our case, as stated in the Theorem above, the particular structure of the characteristic function does not allow an imaginary root with a multiplicity larger than 2. For a deeper discussion on generic maximal multiplicity of a real characteristic root and its properties, the reader is referred to [40].* □

In Fig. 3, the real part of the rightmost root of (19), obtained after elimination of the assigned double root and denoted by γ, is shown with respect to ζ and selected k_1, k_2. As can be seen, the double-root DR (drDR) may become unstable ($\gamma > 0$) for some of the settings. This does not happen e.g. for the smallest possible delays $k_1 = 1$, $k_2 = 2$.

Remark 4. *For the physical implementation, the dimensionless form of the whole resonator feedback needs to be turned to the dimensional form. Considering (7) and (16), it reads as*

$$\bar{u}_a(\vartheta) = -h\ddot{\bar{x}}_a(\vartheta) + \int_0^\vartheta \bar{\alpha}_0 \ddot{\bar{x}}_a(\eta) + \bar{\alpha}_1 \ddot{\bar{x}}_a(\eta - \bar{\tau}_1) + \bar{\alpha}_2 \ddot{\bar{x}}_a(\eta - \bar{\tau}_2) \, \mathrm{d}\eta \qquad (27)$$
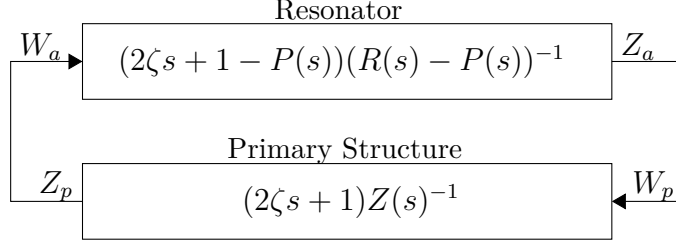
9

Figure 4: A feedback interconnection interpretation of the coupling between absorber and primary structure.

where

$$\bar{\tau}_i = \frac{1}{\Omega}\tau_i, \quad i = 1, 2, \tag{28}$$

and

$$\bar{\alpha}_j = (\bar{m}_a + h)\Omega\alpha_j, \ j = 0..2. \tag{29}$$

$\square$

3.2. Instability of the DR due to a double root assignment

We give some intuition why the inclusion of a (robust) delayed resonator might negatively affect the stability of the overall set-up, which motivates us to include the additional active control (10) of the primary structure.

With $F \equiv 0$ and $U_p \equiv 0$, the combined system can be interpreted as a feedback interconnection of system

$$\begin{cases} (R(s) - P(s)) \ X_a(s) &= W_a(s) \\ Z_a(s) &= (2\zeta s + 1 - P(s))X_a(s) \end{cases} \tag{30}$$

and system

$$\begin{cases} Z(s) \ X_p(s) &= W_p(s) \\ Z_p(s) &= (2\zeta s + 1)X_p(s), \end{cases} \tag{31}$$

where $W_a(s)$ and $W_p(s)$ represent virtual input forces, while $Z_a(s)$ and $Z_p(s)$ represent virtual measurements. The coupling between both (sub)systems, which are well posed, is described by $W_a(s) = Z_p(s)$, $W_p(s) = Z_a(s)$, see Fig. 4. It should be noted that this decomposition is quite natural. For $W_a(s) \equiv 0$ the state equation of system (30) corresponds to the dynamics of the resonator when the primary structure is fixed ($X_p(s) \equiv 0$). Its characteristic equation is given by

$$\det (R(s) - P(s)) = 0, \tag{32}$$

showing the influence of the active control. Similarly, assuming zero input the state equation of system (31) describes the dynamics of the primary structure when the absorber's position is fixed. Hence, the characteristic equation $\det (Z(s)) = 0$ is in accordance with the presence of two spring-damper combinations.

For $P(s) \equiv 0$ both subsystems depicted in Fig. 4 are exponentially stable provided $\zeta > 0$ and $c_p > 0$. When the active resonator feedback is determined to assign simple zeros $\pm j$ to the transfer function from f to x_p, these zeros appear as solutions of (32). Hence, the upper subsystem is not anymore exponentially stable, but still stable in the sense of

Lyapunov. If the overall system is exponentially stable, the lower subsystem can be seen as taking the role of a stabilizing controller for the upper subsystem. Thus, the degree of instability induced by the active feedback of the delayed resonator is compensated by the stability of the primary structure and/or the coupling.

When double zeros are assigned by the resonator feedback, these appear as double non-semisimple eigenvalues of the upper subsystem in Fig. 4, which becomes polynomially unstable (modes of the form $c_1 t \cos(t) + c_2 t \sin(t)$). In such a situation, the stabilization task and the subsequent task of having the closed-loop spectrum sufficiently bounded away from the imaginary axis are much more difficult. This argument, as well as numerical experiments demonstrating a potential loss of stability, lead us to supplement the scheme with active feedback of the primary structure.

3.3. Stabilizing the overall set-up

The absorber and primary structure coupled together, as given by (4), can be described as

$$
\begin{cases}
\dot{x}(t) & = Ax(t) + B_1 u_a(t) + B_2 u_p(t) + B_3 f(t), \\
y_a(t) & = C_a \dot{x}(t) \\
& = C_a Ax(t) + C_a B_1 u_a(t) + C_a B_2 u_p(t) + C_a B_3 f(t), \\
y_p(t) & = C_p x(t),
\end{cases}
\tag{33}
$$

where the output y_a is the measured acceleration $y_a = \ddot{x}_a$, and matrices I, A, B_1, B_2, B_3 correspond to a linear model of a mechanical system (4) with a state vector $x = [x_a \ \dot{x}_a \ x_p \ \dot{x}_p]^T$. Matrix $C_a = [0\ 1\ 0\ 0]$ defines the measured acceleration of the absorber, and $C_p = [0\ 0\ 1\ 0]$ determines the control system output $y_p = x_p$. Concerning the resonator feedback (16), it can be turned to

$$
\dot{u}_a(t) = \alpha_0 y_a(t) + \alpha_1 y_a(t - \tau_1) + \alpha_2 y_a(t - \tau_2).
\tag{34}
$$

System (33) and resonator feedback (34) can be recast into a Delay Differential Algebraic Equations (DDAE) description of the form

$$
\mathbf{E}\dot{\xi}(t) = \mathbf{A_0}\xi(t) + \sum_{i=1}^{2} \mathbf{A}_i \xi(t - \tau_i) + \mathbf{B}_0 f(t) + \mathbf{B}_1 u_p(t),
$$

$$
\mathbf{Y}(t) = \mathbf{C}\xi(t),
\tag{35}
$$

where $\xi = [x^T \quad u_a \quad y_a \quad y_p]^T$ is the (pseudo)state vector, $\mathbf{E} = \mathrm{diag}(I, 1, 0, 0)$, and $\mathbf{Y}(t) = y_p(t)$.

In order to stabilize and optimize the spectrum of the resulting infinite dimensional system, following the methodology proposed in [42], we consider a fixed k^{th}-order dynamic feedback controller in the form

$$
K : \begin{cases}
\dot{x}_K(t) = A_K x_K(t) + B_K y_p(t), \\
u_p(t) = C_K x_K(t) + D_K y_p(t).
\end{cases}
\tag{36}
$$

To assure the system is stable with sufficiently large margin and to avoid undesirably long transients, we design the controller based on minimizing the *spectral abscissa* over the free parameters, i.e. the elements of matrices (A_K, B_K, C_K, D_K). This objective function is defined as

$$
\gamma(K) := \sup\left(\Re(s) : s \in \Sigma(K)\right),
\tag{37}
$$

where $\Sigma(K)$ denotes the spectrum of the closed loop system (35)–(36). For its optimization we use the algorithm and software described in [42].

Let us remark that even in the ideal case where both the DR and main structure are stable, there is no guarantee that their interconnection is stable. Thus application of a stabilizing controller proposed above may be needed also when a classical (quasi-stable) DR is deployed.

Remark 5. *For the physical implementation, the dimensional form of* (36) *turns into*

$$\overline{K} : \begin{cases} \dot{\overline{x}}_K(\vartheta) = \overline{A}_K \overline{x}_K(\vartheta) + \overline{B}_K \overline{y}_p(\vartheta), \\ \overline{u}_p(\vartheta) = \overline{C}_K \overline{x}_K(\vartheta) + \overline{D}_K \overline{y}_p(\vartheta), \end{cases} \tag{38}$$

where $\overline{A}_K = A_K \Omega$, $\overline{B}_K = B_K \Omega$, $\overline{C}_K = C_K \overline{m}_a \Omega^2$, and $\overline{D}_K = D_K \overline{m}_a \Omega^2$ are the corresponding matrices of the controller. □

Remark 6. *For the comparison, we present the alternative robust resonator feedback form proposed in [38] and outline its optimization based design procedure. The resonator feedback is considered in the form*

$$\overline{u}_a(\vartheta) = -h\ddot{\overline{x}}_a(\vartheta) + \int_0^{\overline{\tau}} g(\eta)\ddot{\overline{x}}_a(\vartheta - \eta) \, \mathrm{d}\eta, \tag{39}$$

where the delay distribution function is in the polynomial form

$$g(\eta) = \sum_{i=0}^{N} a_i \eta^i \mathrm{e}^{-\lambda\eta}, \tag{40}$$

with parameters a_i and delay length $\overline{\tau}$. Note that the function $\mathrm{e}^{-\lambda\eta}$ with $\lambda > 0$ is included due to implementation of the delay.

The required widening of the frequency stop band is achieved in [38] by minimizing the squared transmissibility function in the vicinity of the target frequency. Prefixing the delay length $\overline{\tau}$, it leads to solving the Quadratic optimisation problem over $N + 1$ parameter set $p = [a_0, a_1, ..a_N]^T$. However, due to destabilizing effect of the robustified DR, the optimization problem was extended by including the stability constraint $\overline{\gamma}(p) < 0$, where $\overline{\gamma}(p)$ denotes the spectral abscissa of the whole system. Applying the penalty method, the constrained quadratic optimization problem is turned to an unconstrained nonlinear optimization problem. In the case study section of [38], the problem was successfully solved by HANSO (Hybrid Algorithm for Nonsmooth Optimization) [48]. Note that HANSO is also involved in the software tool [42] used to design the controller (36). □

4. Case study validation

The validation is performed both by simulations and experiments. For the purpose of the latter, an experimental set-up has been built, which is shown in Fig. 5 together with implementation of the control scheme. The set-up built according to the scheme in Fig. 1 consists of two carts. The absorber cart $(\overline{m}_a)$ is interconnected with the primary structure cart $(\overline{m}_p)$ by a pair of springs. Another pair of springs is used to fix the primary structure cart to the left and right base elements. Both the carts slide on rails - the absorber-rails

are fixed to the primary structure while the primary-rails are fixed to the base. The carts are actuated by two voice-coil linear motors generating forces $\bar{u}_a$ and $\bar{u}_p$. The damping in the connecting links is mainly due to viscous friction between the bearings and the rails. The position $\bar{x}_p$ of the primary structure is measured by an incremental position sensor while acceleration of the absorber $\ddot{\bar{x}}_a$ is measured by an accelerometer. The proposed control scheme consists of the resonator feedback (16) and the stabilizing controller (36).

Concerning the hardware implementation visualized in Fig. 5, the excitation of the primary structure is performed via the voice coil linear motor (AVM40-20-0.5, with continuous force $9.93\,\mathrm{N}$) connecting the primary with the base. The absorber is actuated by a second voice coil (LVCM-032-076-02, with continuous force $8\,\mathrm{N}$), which is placed between the primary structure and the absorber. The control algorithms (27) and (38) are implemented in LabVIEW™ and performed using the CompactRIO controller with $1\,\mathrm{kHz}$ sampling. Note that Euler explicit method was used for solving both (27) and (38). FPGA module of CompactRIO is responsible for fast sensor measurement, particularly from the incremental position sensor requiring fast quadrature encoder signal. Additionally, the CompactRIO controller is equipped with the three additional modules. The first, NI-9870 module communicates by RS-232 bus with instrument control unit (ICU) which translates commands into electric current forcing both voice coils to move (with current/torque control loop). The second, NI-9401 module, detects pulses of the quadrature signal generated by the incremental position sensor AS5304 during its motion. The AS5304 is a sensor with integrated Hall elements for measuring linear motion using a multi-pole magnetic strip placed on the base alongside the main rail. The resolution of the position measurement is $25\,\mathrm{\mu m}$. The last one is the NI-9230 module, which is designed to measure signals from both the integrated electronic piezoelectric (IEPE) type sensors and non IEPE type sensors. A miniature piezoelectric accelerometer KS95B.100 with high resonant frequency is connected to the module and measures acceleration of the absorber.

The parameters of the system according to Fig. 1 identified on the set-up are given as follows: $\bar{m}_a = 0.52\,\mathrm{kg}$, $\bar{c}_a = 1.45\,\mathrm{N\,s\,m^{-1}}$, $\bar{k}_a = 418.50\,\mathrm{N\,m^{-1}}$, $\bar{m}_p = 1.157\,\mathrm{kg}$, $\bar{c}_p = 3.92\,\mathrm{N\,s\,m^{-1}}$, $\bar{k}_p = 1503.30\,\mathrm{N\,m^{-1}}$. The absorber damping and natural frequency are then given as $\Omega = 28.37\,\mathrm{s^{-1}}$ and $\zeta = 0.0491$. The excitation frequency of the force $\bar{f}$ acting on the primary structure is selected to be identical with Ω, i.e. $\bar{\omega}_f = 28.37\,\mathrm{s^{-1}}$. Thus, the parameters in the dimensionless model (4) with $\omega_f = 1$ are given as $\zeta = 0.0491$, $m_p = 2.225, c_p = 0.2657, k_p = 3.592$. Let us mention that when the excitation frequency need be shifted, the absorber mass can be easily adjusted according to (6) by selecting appropriate number and weight of the steel plates seen in the top of the absorber in Fig. 5. Alternatively, the virtual mass adjustment can be performed by including delay free acceleration feedback (7) with h determined by (8), as proposed in [22].

For parametrization of the robust resonator with the delay distribution given by (18), Theorem 1 is applied. Selecting $k_1 = 1, k_2 = 2$, implies by (20) $\tau_1 = \pi, \tau_2 = 2\pi$, $\alpha_0 = 0.3920, \alpha_1 = -0.0491, \alpha_2 = -0.3429$ ($\bar{\tau}_1 = 0.1107\,\mathrm{s}, \bar{\tau}_2 = 0.2215\,\mathrm{s}, \bar{\alpha}_0 = 5.7832\,\mathrm{kgs^{-1}}, \bar{\alpha}_1 = -0.7250\,\mathrm{kgs^{-1}}, \bar{\alpha}_2 = -5.0582\,\mathrm{kgs^{-1}}$). Applying the QPmR algorithm [49], the rightmost spectrum of the retarded characteristic equation (19) is shown in Fig. 6. Next to the spectrum values denoted as black dots, the iso-lines $\Re(M(s)) = 0$ (solid) and $\Im(M(s)) = 0$ (dashed) are shown. The root multiplicity two at $s = j$ is confirmed by two couples of $\Re(M(s)) = 0$ and $\Im(M(s)) = 0$ iso-lines intersecting at this point, see [49]. As can be seen from the figure, the given roots $s_{1,2,3,4}$ are the rightmost roots.

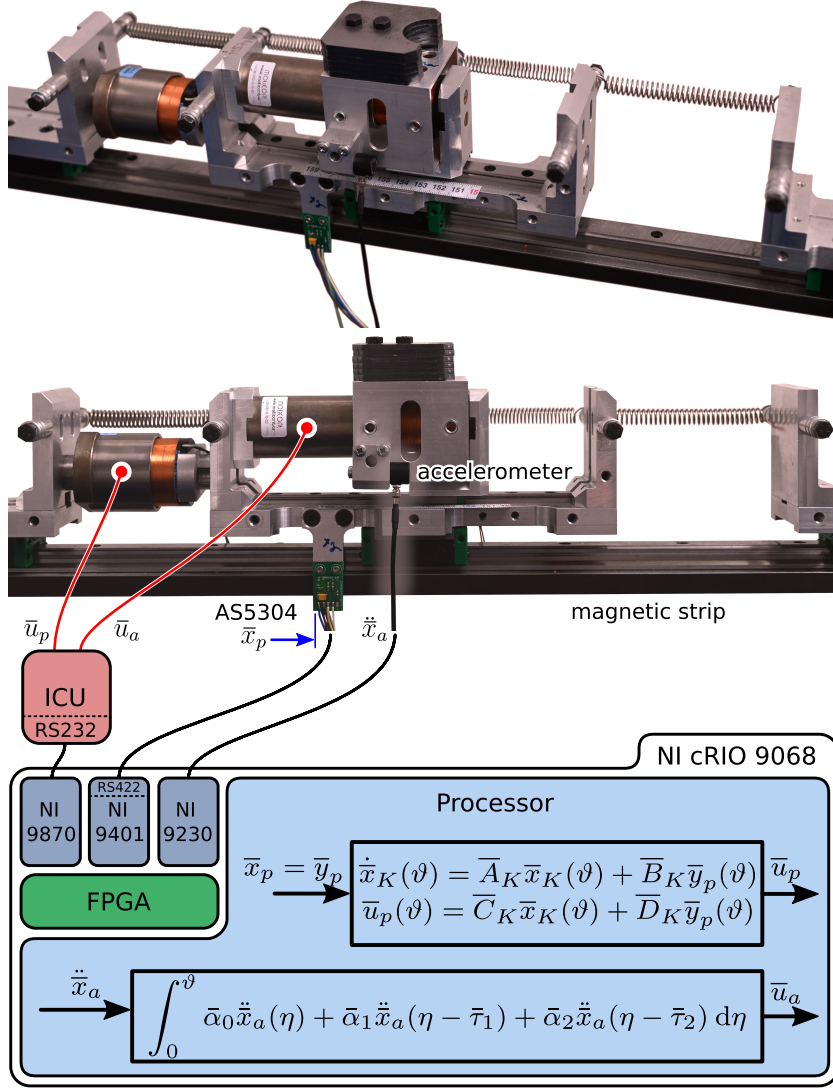In Fig. 7, the spectrum of the *double root* delayed resonator (drDR) (3) and (16), as

Figure 5: Experimental setup built according to Fig. 1 controlled by NI CompactRIO, where the control algorithms (7) and (36) are implemented in LabVIEW™.

well as the spectrum of its coupling with the primary structure (4) and (16) are shown. As can be seen, the spectrum of the interconnected system is unstable. Thus, the controller (36) of the order $k = 2$ is tuned by minimising the system spectral abscissa [42], leading to

$$A_K = \begin{bmatrix} 0.1956 & 1.0532 \\ -1.1881 & -1.0502 \end{bmatrix}, \quad B_K = \begin{bmatrix} 0.9371 \\ 0.4681 \end{bmatrix},$$
$$C_K = \begin{bmatrix} 1.2523 & -0.0416 \end{bmatrix}, \quad D_K = \begin{bmatrix} -0.1992 \end{bmatrix}, \tag{41}$$

which in the dimensional form reads as

$$\overline{A}_K = \begin{bmatrix} 5.5491 & 29.8774 \\ -33.7047 & -29.7933 \end{bmatrix}, \quad \overline{B}_K = \begin{bmatrix} 26.5854 \\ 13.2788 \end{bmatrix},$$
$$\overline{C}_K = \begin{bmatrix} 524.0673 & -17.4006 \end{bmatrix}, \quad \overline{D}_K = \begin{bmatrix} -83.3501 \end{bmatrix}, \tag{42}$$

respectively.

As shown in Fig. 7, the drDR with the controlled primary structure is stable with spectral abscissa $\gamma = -0.1046$ ($\bar{\gamma} = -2.9675\,\mathrm{s}^{-1}$).
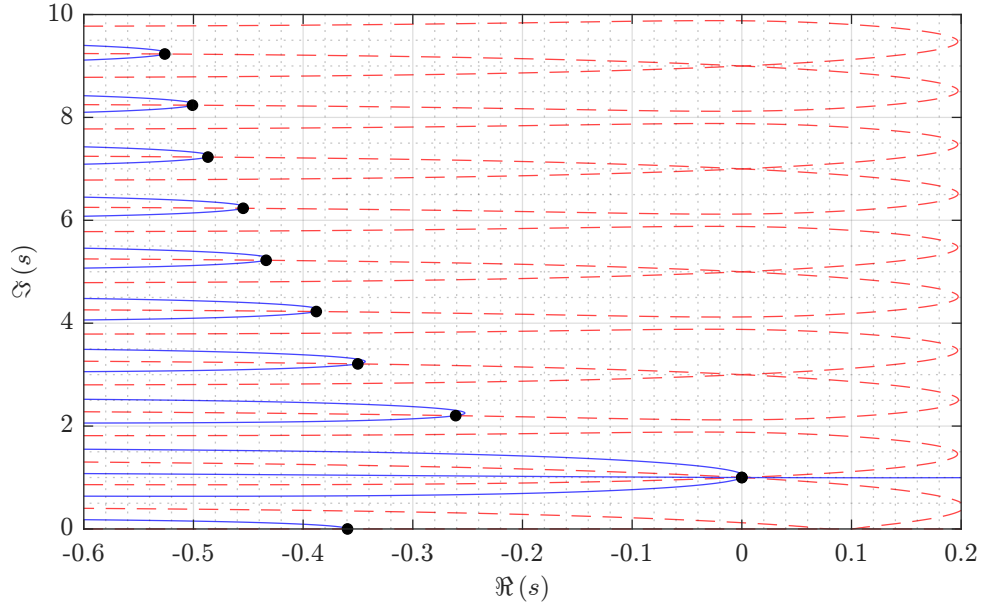
14

Figure 6: Rightmost spectrum of characteristic equation (19), parameterized by Theorem 1 considering $\zeta = 0.0491, k_1 = 1, k_2 = 2$: black dots - roots, solid iso-line - $\Re(M(s)) = 0$, dashed iso-line - $\Im(M(s)) = 0$ (results shown for scaled parameters).
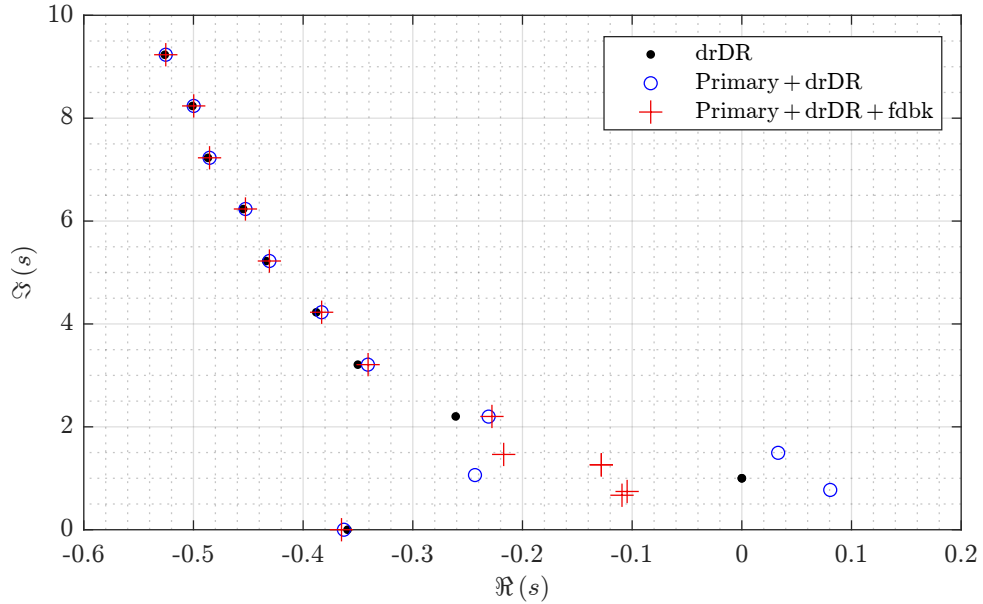

Figure 7: Spectra of the drDR, (3) and (16), alone, drDR - primary structure interconnection, (4) and (16), without the controller (unstable), and with the controller (36) (stable) (results shown for scaled parameters).
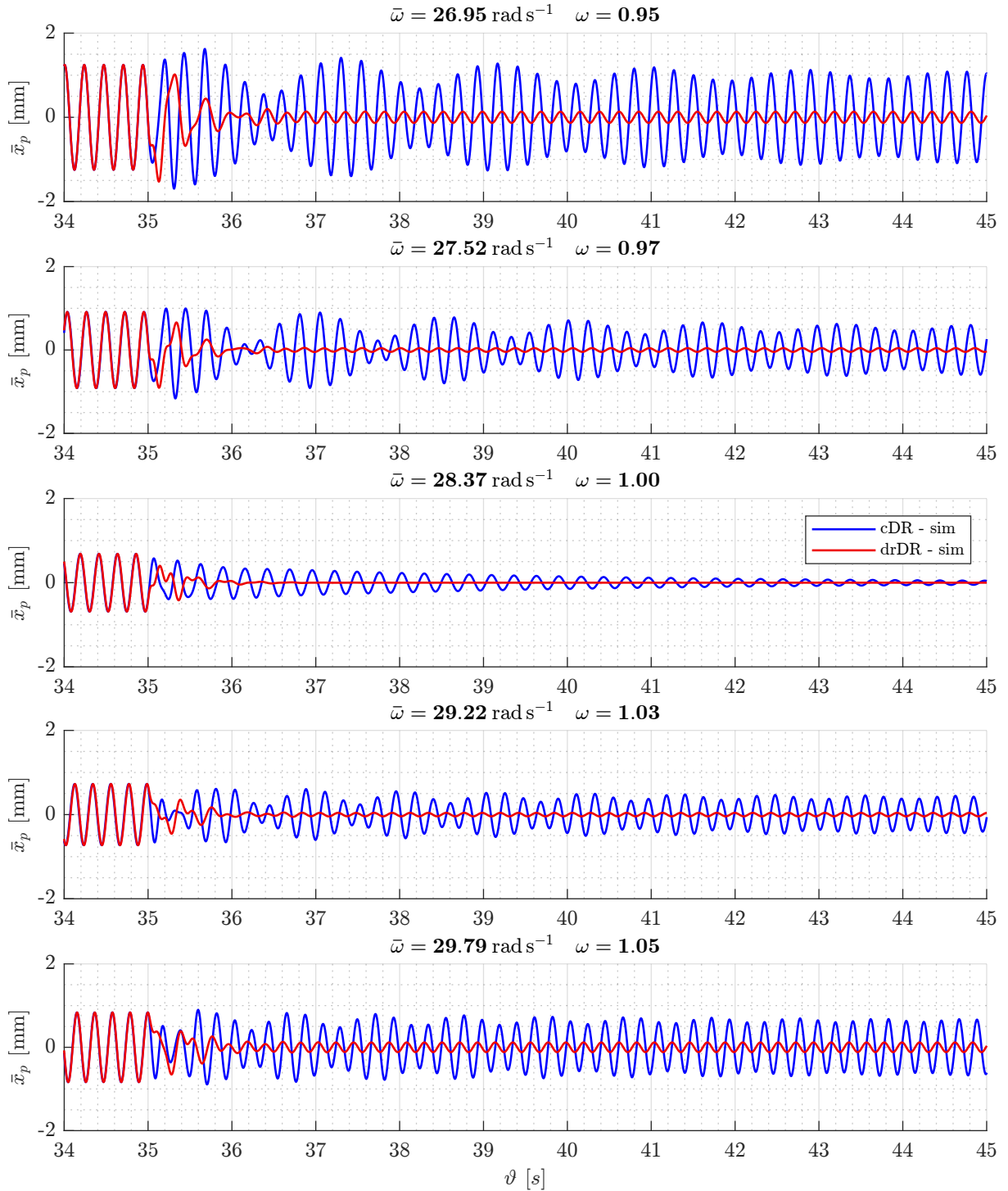
Figure 8: Simulation results of DRs performance at five excitation frequencies, considering $\bar{\omega} = \bar{\omega}_f (1 + \delta)$ in (1). The DR feedback and stabilization switched on at $t = 3\,\mathrm{s}$.
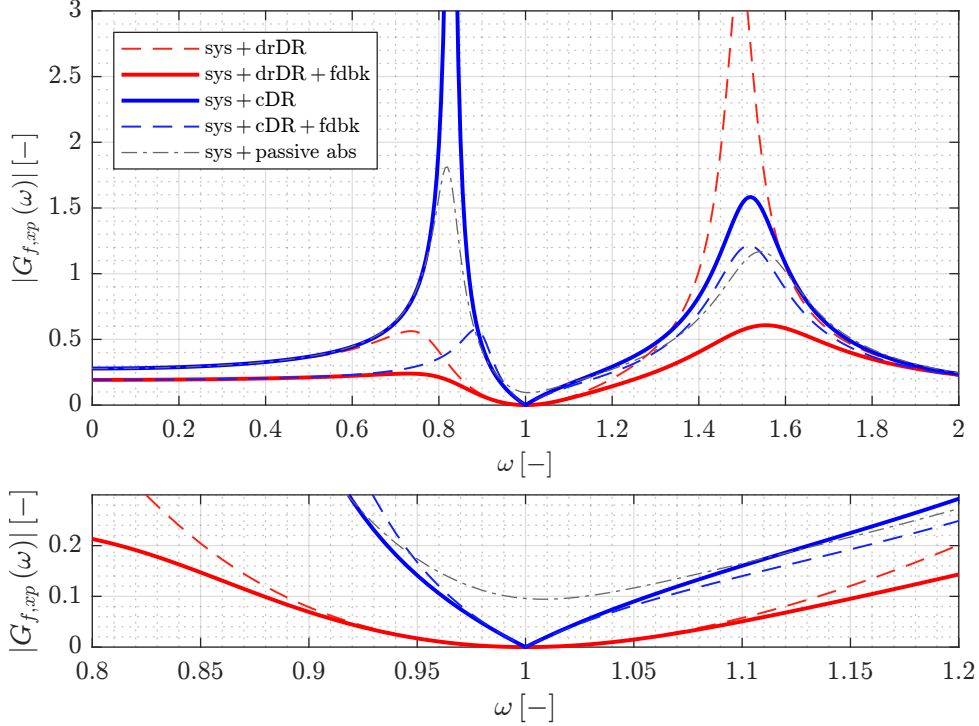
Figure 9: Magnitude of the transfer function $G_{f,x_p}(j\omega)$ given by (12) with: i) drDR and the stabilizing controller, and ii) cDR (results shown for scaled parameters).

In the next step, the performance validation is done via simulations. Next to the nominal excitation frequency $\omega_f = 1$ case, the setting with 3% ($\delta = \pm 0.03$) and 5% ($\delta = \pm 0.05$) mismatch between the design and true excitation frequencies are considered to study the robustness. Considering $\bar{\omega} = \bar{\omega}_f(1 + \delta)$ in the excitation force (1), the absorption robustness is studied for $\bar{\omega} = 26.95\,\mathrm{s}^{-1}$ ($\delta = -0.05$), $\bar{\omega} = 27.52\,\mathrm{s}^{-1}$ ($\delta = -0.03$), $\bar{\omega} = 28.37\,\mathrm{s}^{-1}$ ($\delta = 0$), $\bar{\omega} = 29.22\,\mathrm{s}^{-1}$ ($\delta = 0.03$) and $\bar{\omega} = 29.79\,\mathrm{s}^{-1}$ ($\delta = 0.05$). For comparison, results of a *classical* delayed resonator (cDR) with lumped delay feedback, in dimensionless form given by

$$u_a(t) = g_{cDR}\ddot{x}_a(t - \tau_{cDR}), \tag{43}$$

and in dimensional form by

$$\bar{u}_a(\vartheta) = \bar{g}_{cDR}\ddot{\bar{x}}_a(\vartheta - \bar{\tau}_{cDR}), \tag{44}$$

respectively, are shown, with gain $g_{cDR} = 2\zeta = 0.0982$ and time delay $\tau_{cDR} = \frac{\pi}{2}$ ($\bar{g}_{cDR} = \bar{m}_a g_{cDR} = 0.0511\,\mathrm{kg}$, $\bar{\tau}_{cDR} = 0.0554\,\mathrm{s}$), parametrized by assigning a single root pair $s_{1,2} = \pm j$ ($\bar{s}_{1,2} = \pm j28.37$) to the delayed resonator [5]. From the results shown in Fig. 8, it can be seen that for nominal frequency $\omega = 1$ ($\bar{\omega} = 28.37\,\mathrm{s}^{-1}$) both DRs perform well. However, for the cases with the 3% and 5% frequency mismatch, the drDR performs considerably better with substantially smaller residual vibration amplitudes.

Subsequently, the enhancement of the robustness is studied via the magnitudes of the frequency responses $|G_{f,x_p}(j\omega)|$ of the transfer function (12) between the excitation force f and the position of the primary x_p. If the cDR (43) is applied, then $|G_{f,x_p}(j\omega)|$ goes to zero for the nominal frequency $\omega = 1$ as shown in Fig. 9. For the frequencies in the vicinity of $\omega = 1$, this function tends to rapidly increase and therefore, if there
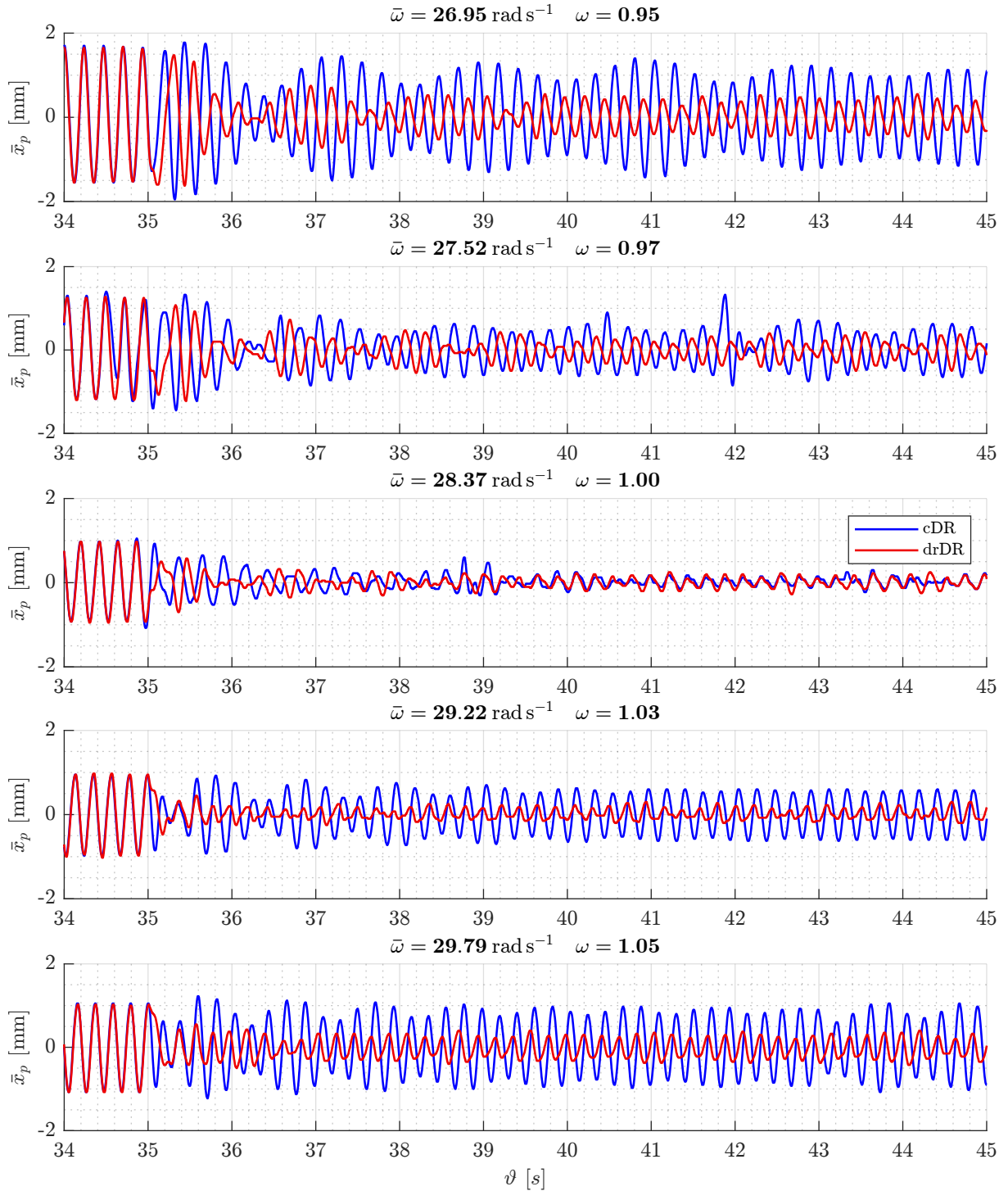
17

Figure 10: Experimental results of DRs performance at five excitation frequencies, considering $\bar{\omega} = \bar{\omega}_f(1 + \delta)$ in (1). The DR feedback and stabilization switched on at $t = 3\,\mathrm{s}$.

is an uncertainty in the excitation frequency, the quality of the vibration suppression is likely to decay. On the other hand, the $|G_{f,x_p}(j\omega)|$ magnitude with drDR and stabilizing feedback has parabolic shape in the vicinity of $\omega = 1$ with considerably smaller increase in its neighborhood, compared to the cDR. Another positive aspect of the given solution is considerably lower H_∞ norm (maximum of the frequency response magnitude) when the stabilizing controller is applied, compared to cDR case without the controller. Though, a positive impact of the controller is observed when it is used together with the cDR as it lowers the H_∞ norm substantially also for this case. For the demonstration purposes, in Fig. 9, we also show the amplitude of the drDR without the stabilizing feedback. As can be seen, the H_∞ norm increases substantially, although the characteristics close to the target frequency remained unchanged. This confirms the fact that the robustness in vibration suppression is truly imposed by the drDR.

Finally, the experimental validation is performed analogously to the simulation result set shown in Fig. 8. The experimental results are shown in Fig. 10[2]. As can be seen, considerably better robustness in vibration suppression is confirmed for the drDR. For the 3% and 5% mismatch between true and design excitation frequencies, considerable smaller amplitudes can be observed for the results by drDR compared to the results by cDR. Note that compared to the simulation results, certain residual vibration can be observed for the nominal frequency ($\delta = 0$). The most likely reason is in the considerable measurement noise of the accelerometer. Besides, the unmodelled nonlinear dynamics (mainly due to the Coulomb friction) could negatively contribute to the physical drDR(cDR)'s performance decay. However, despite to this imperfection, it can be concluded that the main objective of the experimental validation of robustness enhancement due to drDR application has been fulfilled.

To conclude, let us discuss briefly the results against those achieved in simulation case study of [38]. Let us note that in [38] only a single actuator is considered governed by (39), i.e. with $\bar{u}_p = 0$. Applying the complex optimization based design, analogous results in vibration suppression robustness were achieved in [38] as in the above case study with simple structure drDR feedback, though with slight residual vibration for the nominal frequency. However, including the stability condition did not have such a positive effect on overall H_∞ norm, which is observed in the current set-up with a separate stabilizing controller.

5. Conclusions

A robust version of the delayed resonator with acceleration feedback for vibration suppression is proposed as the main result. The resonator feedback is in a form of distributed delay which is composed of two segments. The length of the segments and the gains are determined utilizing recent analytical results on admissible multiplicity of fixed structure delay systems. An enhanced attention is paid to stability aspects of both the isolated resonator and the overall system, i.e. the resonator deployed at the primary structure to be silenced. It is shown that the double root placed at the imaginary axis destabilizes the resonator, independently of the location of its other roots in the infinite spectrum. This is likely to have negative consequences for the stability of the overall system. To handle this risky feature, the control scheme is supplemented by a stabilizing finite order

---

[2]Video record of the experiments is shown at https://control.fs.cvut.cz/en/aclab/experiments/robustdr

controller acting at the primary structure. The controller parameters are determined by an optimization method with the objective to minimize the spectral abscissa of the overall control scheme formulated as an interconnected time delay system.

The proposed robust vibration absorption method is thoroughly validated on an extensive case study. First, the numerical and simulation based analysis is performed on a model of the physical laboratory set-up which is proposed and built for that purpose. The enhanced robustness in vibration absorption is then confirmed by both simulations and experiments. The case study analysis also revealed positive effect of the stabilizing feedback on the robustness of the overall control scheme. For the experimental validation the control algorithms were implemented in LabVIEW™ and ran on the NI CompactRIO hardware.

Even though the presented results proved conceptual applicability of the proposed vibration suppression method with enhanced robustness against frequency mismatch, one has to take into account the assumptions that need to be fulfilled and technical limitations. First of all, for tuning the parameters of the absorber feedback, a very precise mathematical model of the absorber needs to be available. As a rule, determining the absorber mass and link stiffness are relatively easy tasks. However, as a rule, it is not the case for the damping. In our configuration of the set-up, for example, the damping forces are composed of inherent damping of the springs and the friction of the bearings, which is temperature dependent and is likely to vary in time. Another limitation comes from the well-known fact that even though the active feedback and/or mechanical adjustment of some of the physical parameters (mass in our example) can extend the applicable frequency range, it still has some relatively strict limits due to mechanical construction of the absorber, which remains fixed. Let us also mention that the proposed two step control feedback design where the vibration absorption and stabilization tasks are handled separately does not need to lead to an optimal solution, e.g. with respect to the overall energy needed for the control.

Motivated by the above outlined imperfections and limitations, in the subsequent research, methods to further enhance the vibration suppression quality, robustness in both vibration suppression and stability will be investigated. It will include an application of filtration techniques to handle the noise of the accelerometer sensors and algorithms to compensate for the inherent nonlinearities such as Coulomb friction. On the construction side of the mechatronic absorber, the current bearings will be substituted by low-friction bearings. In the control design research direction, the attention will be paid to simultaneous design of the active absorber and the resonator, targeting multiple frequencies and non-collocated vibration suppression.

References

[1] A. Preumont, Vibration control of active structures: an introduction, Vol. 246, Springer, 2018.

[2] R. Rana, T. Soong, Parametric study and simplified design of tuned mass dampers, Engineering structures 20 (3) (1998) 193–204.

[3] G.-L. Lin, C.-C. Lin, B.-C. Chen, T.-T. Soong, Vibration control performance of tuned mass dampers with resettable variable stiffness, Engineering Structures 83 (2015) 187–197.

[4] P. Gao, C. Xiang, H. Liu, P. Walker, N. Zhang, Design of the frequency tuning scheme for a semi-active vibration absorber, Mechanism and Machine Theory 140 (2019) 641–653.

[5] N. Olgac, B. Holm-Hansen, A novel active vibration absorption technique: delayed resonator, Journal of Sound and Vibration 176 (1) (1994) 93–104.

[6] N. Olgac, B. Holm-Hansen, Tunable active vibration absorber: the delayed resonator, Journal of dynamic systems, measurement, and control 117 (4) (1995) 513–519.

[7] N. Olgac, M. Hosek, Active vibration absorption using delayed resonator with relative position measurement, Journal of vibration and acoustics 119 (1) (1997) 131–136.

[8] M. Hosek, H. Elmali, N. Olgac, A tunable torsional vibration absorber: the centrifugal delayed resonator, Journal of Sound and Vibration 205 (2) (1997) 151–165.

[9] D. Filipovic, N. Olgac, Torsional delayed resonator with velocity feedback, IEEE/ASME transactions on mechatronics 3 (1) (1998) 67–72.

[10] D. Filipović, N. Olgac, Delayed resonator with speed feedback–design and performance analysis, Mechatronics 12 (3) (2002) 393–413.

[11] N. Olgac, H. Elmali, M. Hosek, M. Renzulli, Active vibration control of distributed systems using delayed resonator with acceleration feedback, Journal of dynamic systems, measurement, and control 119 (3) (1997) 380–389.

[12] N. Jalili, N. Olgac, Multiple delayed resonator vibration absorbers for multi-degree-of-freedom mechanical structures, Journal of Sound and Vibration 223 (4) (1999) 567–585.

[13] M. E. Renzulli, R. Ghosh-Roy, N. Olgac, Robust control of the delayed resonator vibration absorber, Control Systems Technology, IEEE Transactions on 7 (6) (1999) 683–691.

[14] M. Hosek, N. Olgac, A single-step automatic tuning algorithm for the delayed resonator vibration absorber, Mechatronics, IEEE/ASME Transactions on 7 (2) (2002) 245–255.

[15] N. Jalili, N. Olgac, Identification and retuning of optimum delayed feedback vibration absorber, Journal of guidance, control, and dynamics 23 (6) (2000) 961–970.

[16] N. Jalili, N. Olgac, A sensitivity study on optimum delayed feedback vibration absorber, J. Dyn. Sys., Meas., Control 122 (2) (2000) 314–321.

[17] T. Vyhlídal, N. Olgac, V. Kučera, Delayed resonator with acceleration feedback–complete stability analysis by spectral methods and vibration absorber design, Journal of Sound and Vibration 333 (25) (2014) 6781–6795.

[18] J. K. Hale, S. V. Lunel, Introduction to functional differential equations, Springer-Verlag, New York, 1993.

[19] W. Michiels, S.-I. Niculescu, Stability, Control, and Computation for Time-Delay Systems: An Eigenvalue-Based Approach, Vol. 27, SIAM, 2014.

[20] D. Pilbauer, T. Vyhlídal, N. Olgac, Delayed resonator with distributed delay in acceleration feedback - design and experimental verification, IEEE/ASME Transactions on Mechatronics 21 (4) (2016) 2120–2131. `doi:10.1109/TMECH.2016.2516763`.

[21] N. Olgac, R. Sipahi, The cluster treatment of characteristic roots and the neutral type time-delayed systems, Journal of dynamic systems, measurement, and control 127 (1) (2005) 88–97.

[22] V. Kučera, D. Pilbauer, T. Vyhlídal, N. Olgac, Extended delayed resonators–design and experimental verification, Mechatronics 41 (2017) 29–44.

[23] Q. Gao, Y. Liu, J. Cai, H. Wu, Z. Long, Complete stability analysis and optimization of the extended delayed resonator with virtual natural frequency adjustment, Journal of Dynamic Systems, Measurement, and Control 145 (1) (2023) 011002.

[24] T. Vyhlídal, D. Pilbauer, B. Alikoç, W. Michiels, Analysis and design aspects of delayed resonator absorber with position, velocity or acceleration feedback, Journal of Sound and Vibration 459 (2019) 114831.

[25] A. S. K. Kammer, N. Olgac, Electromechanical delayed resonator implementation using piezoelectric networks, in: Proceedings of the 13th IFAC Workshop on Time-Delay Systems, 2016, pp. 71–76. `doi:10.1016/j.ifacol.2016.07.475`.

[26] N. Olgac, R. Jenkins, Actively tuned noncollocated vibration absorption: An unexplored venue in vibration science and a benchmark problem, IEEE Transactions on Control Systems Technology 29 (1) (2020) 294–304.

[27] R. Jenkins, N. Olgac, Real-time tuning of delayed resonator-based absorbers for spectral and spatial variations, Journal of Vibration and Acoustics 141 (2) (2019).

[28] Y. Liu, J. Cai, N. Olgac, Q. Gao, A robust delayed resonator construction using amplifying mechanism, Journal of Vibration and Acoustics 145 (1) (2023) 011010.

[29] J. Cai, Y. Liu, Q. Gao, Y. Chen, Spectrum-based stability analysis for fractional-order delayed resonator with order scheduling, Journal of Sound and Vibration 546 (2023) 117440.

[30] O. Eris, B. Alikoc, A. F. Ergenc, A new delayed resonator design approach for extended operable frequency range, Journal of Vibration and Acoustics 140 (4) (2018) 041003.

[31] M. Valášek, N. Olgac, Z. Neusser, Real-time tunable single-degree of freedom, multiple-frequency vibration absorber, Mechanical Systems and Signal Processing 133 (2019) 106244.

[32] T. Vyhlídal, W. Michiels, Z. Neusser, J. Bušek, Z. Šika, Analysis and optimized design of an actively controlled two-dimensional delayed resonator, Mechanical Systems and Signal Processing 178 (2022) 109195.

[33] Z. Šika, T. Vyhlídal, Z. Neusser, Two-dimensional delayed resonator for entire vibration absorption, Journal of Sound and Vibration 500 (2021) 116010.

[34] L. Hernández-Villa, D. Melchor-Aguilar, On stability of sdof systems with delayed position and velocity feedback, Journal of Vibration and Control (2022) 10775463221100065.

[35] H. Rivaz, R. Rohling, An active dynamic vibration absorber for a hand-held vibroelastography probe, Journal of Vibration and Acoustics 129 (1) (2007) 101–112.

[36] N. Alujević, I. Tomac, P. Gardonio, Tuneable vibration absorber using acceleration and displacement feedback, Journal of sound and vibration 331 (12) (2012) 2713–2728.

[37] S. Mohanty, S. Dwivedy, Linear and nonlinear analysis of piezoelectric based vibration absorber with acceleration feedback, Procedia Engineering 144 (2016) 584–591.

[38] D. Pilbauer, T. Vyhlídal, W. Michiels, Optimized design of robust resonator with distributed time-delay, Journal of Sound and Vibration 443 (2019) 576–590.

[39] I. Boussaada, S.-I. Niculescu, Characterizing the codimension of zero singularities for time-delay systems, Acta Applicandae Mathematicae 145 (1) (2016) 47–88.

[40] G. Mazanti, I. Boussaada, S.-I. Niculescu, Multiplicity-induced-dominancy for delay-differential equations of retarded type, Journal of Differential Equations 286 (2021) 84–118.

[41] I. Boussaada, S.-I. Niculescu, Tracking the algebraic multiplicity of crossing imaginary roots for generic quasipolynomials: A vandermonde-based approach, IEEE Transactions on Automatic Control 61 (6) (2015) 1601–1606.

[42] W. Michiels, Spectrum-based stability analysis and stabilisation of systems described by delay differential algebraic equations, IET control theory & applications 5 (16) (2011) 1829–1842. `doi:10.1049/iet-cta.2010.0752`.

[43] P. Appeltans, H. Silm, W. Michiels, Tds-control: a matlab package for the analysis and controller-design of time-delay systems, IFAC-PapersOnLine 55 (16) (2022) 272–277.

[44] M. Kuře, T. Vyhlídal, W. Michiels, I. Boussaada, Spectral design of robust delayed resonator by double-root assignment, IFAC-PapersOnLine 51 (14) (2018) 72–77.

[45] K. Pyragas, Continuous control of chaos by self-controlling feedback, Physics Letters A 170 (1992) 421–428.

[46] H. Huijberts, W. Michiels, H. Nijmeijer, Stabilisability via time-delayed feedback: an eigenvalue optimisation approach, SIAM Journal on Applied Dynamical Systems 8 (1) (2009) 1–20.

[47] G. Pólya, G. Szegö, Problems and Theorems in Analysis II: Theory of Functions. Zeros. Polynomials. Determinants. Number Theory. Geometry, Springer Science & Business Media, 1997.

[48] M. Overton, Hanso: a hybrid algorithm for nonsmooth optimization, Available from cs. nyu. edu/overton/software/hanso (2009).

[49] T. Vyhlidal, P. Zítek, Mapping based algorithm for large-scale computation of quasi-polynomial zeros, IEEE Transactions on Automatic Control 54 (1) (2009) 171–177.